# Two-dimensional nanoplates of $Bi_2Te_3$ and $Bi_2Se_3$ with reduced thermal stability

Cite as: AIP Advances **6**, 025110 (2016); https://doi.org/10.1063/1.4942113
Submitted: 24 December 2015 • Accepted: 04 February 2016 • Published Online: 11 February 2016

Sung Min Kang, Sung-Soo Ha, Wan-Gil Jung, et al.

# Two-dimensional nanoplates of $Bi_2Te_3$ and $Bi_2Se_3$ with reduced thermal stability

Sung Min Kang,[1] Sung-Soo Ha,[2] Wan-Gil Jung,[2] Mansoo Park,[1]
Hyon-Seok Song,[1] Bong-Joong Kim,[2,a] and Jung-Il Hong[1,3,a]
[1]*Department of Emerging Materials Science, DGIST, Daegu, Korea*
[2]*School of Materials Science and Engineering, GIST, Gwangju, Korea*
[3]*Center for Emerging Materials, DGIST, Daegu, Korea*

(Received 24 December 2015; accepted 4 February 2016; published online 11 February 2016)

Free-standing thin nanoplates of $Bi_2Te_3$ and $Bi_2Se_3$ were synthesized by solvothermal method. It was demonstrated that the thickness of the nanoplates can be controlled by introducing a controlled amount of polyvinylpyrrolidone (PVP) in the synthesis reaction. PVP bonds to the polar basal planes of hexagonal crystal structure of $Bi_2Te_3$ and $Bi_2Se_3$, and they suppress the growth (speed) of the hexagonal crystals in the c-axis direction. Highly anisotropic growth yielded the formation of 2-dimensional nanostructures of nanoplates. The plates were examined directly with transmission electron microscopy (TEM) with *in-situ* heating. These crystalline nanoplates with extremely high width to thickness ratios were found to exhibit much lower thermal stability compared to the bulk counterpart or the conventional nanoparticles as represented by the reduced melting temperature. The melting temperature of a nanoplate decreased by more than 100°C compared to the melting temperature of the bulk material. While it is widely known that the meting temperature decreases for nanoparticles with reduced sizees in all three spatial dimensions, we demonstrate that the reduction in one dimension, i.e. thickness of the platelets in the present study, is effective enough to induce much greater decrease of the melting point than the decrease as observed for the case of nanoparticles.  [http://dx.doi.org/10.1063/1.4942113]

Research on nanomaterial emerged naturally along with the worldwide attentions on the nanotechnology during the last two decades. It is generally accepted that nanomaterial should have at least one dimension less than approximately 100 nm. Nanoparticles are considered to be zero dimensional (0D) nanomaterials, and they are heavily studied since the early '90s when the initial stage of nanotechnology begins.[1,2] Then the focus moved to higher dimensional nanomaterials: first one dimensional (1D) nanowires,[3,4] and then to two dimensional (2D) graphene made of carbon atoms.[5] Nowadays, many researchers are making efforts toward the synthesis and applications of 2D nanostructured materials made of non-carbon elements.[6–8] Along these developments, many new and unexpected properties of nanomaterials were discovered, most of which are due to the reduced size of the material under study.[9–11] As the nanomaterial was developed with the change of dimensionality, the corresponding properties should also depend on the dimensionality of the material, which means that the shape of the material affects the physical properties.[12–14] Therefore, the *'shape effect'* in addition to the size effect should be considered in dealing with nanomaterials of various dimensions such as nanoparticles, nanowires, and nanoplates.

With this in consideration, the thickness of the thin nanoplates or 2D nanostructures should be apparently one of the critical factors that determine the overall properties of the nanoplate.[15–17] Therefore, precise control of thickness in the nanometer scale would provide the capability to tailor the physical properties in a desired manner for the technological application of 2D nanomaterials.

[a]Email: kimbj@gist.ac.kr (BJK), jihong@dgist.ac.kr (JIH)

 

In the present work, we attempt to control the thickness of 2D nanoplates of $Bi_2Te_3$ and $Bi_2Se_3$ with the hexagonal crystal structures. As in the case of Wurtzite structured ZnO nanoplate, highly asymmetric nature of the crystal structure is expected to allow the growth of nanomaterial in an asymmetric shape, which is nanoplates in the present study. Therefore, with the layered hexagonal structure of $Bi_2Te_3$ and $Bi_2Se_3$ consisting of stacks of quintuple layers along the *c*-axia direction, it is likely that the nanoplates can successfully synthesized.

As a demonstration of the property change due to the shape, thermal stability of the nanoplates was then tested by directly examining the melting behaviors of nanoplates with transmission electron microscope equipped with an *in-situ* heating stage. Reduced melting temperature of the nanoparticles is an important issue not only from the fundamental point of view but also from the engineering aspect considering the possible applications of nanomaterial for example in the printed electronics technology.[18–20] With the melting behavior of thin nanoplates in the present study, it is demonstrated (for the first time) that the size reduction in only one of the three spatial dimensions is sufficient to induce the significant decrease of the melting temperature.

Bismuth oxide ($Bi_2O_3$, typically 99.99%), tellurium (Te, 99.999%), selenium (Se, 99.999%), ethylene glycol (EG, spectrophotometric grade 99+%), and polyvinylpyrrolidone (PVP, average molecular weight = 58,000) were purchased from Alfa Aesar. All chemicals were used for the synthesis of the $Bi_2Te_3$ and $Bi_2Se_3$ as purchased without further purification. Solvothermal synthesis method was employed for the reactions following the procedures in Ref. 21: Using a stirrer, various amount of PVP ranging from 0.1 to 0.7 mmol was dissolved in 20 ml of EG until the solution is clear. Then, 0.5 mmol of $Bi_2O_3$ powders and 1.5 mmol of Te powders (or Se powders) were added to the solution. The solution was stirred satisfactorily and transferred into a stainless-steel autoclave with Teflon lining (capacity: 50 ml). The sealed autoclave was placed in an oven which had been pre-heated to 200°C. After 24 hours of reaction at 200°C, the autoclave was taken out of the oven and cooled to room temperature. The gray products were collected by centrifugation followed by washing with distilled water and absolute ethanol for three times, respectively. The solution was finally dried in a glove bag with continuous flow of dry nitrogen gas.

Crystal structures of the synthesized $Bi_2Te_3$ and $Bi_2Se_3$ powders were examined using an x-ray diffractometer (PANalytical Empyrean) equipped with Cu x-ray source. Morphologies of the dry powders were imaged with scanning electron microscopy (SEM) and transmission electron microscopy (TEM). *In-situ* TEM observations were carried out as the specimens were heated up to ~500°C.

Thermal properties of the nanoplates were measured with the TG-DTA 8120 model manufactured by Rigaku Inc. Powders were placed in the quartz sample holder and mounted in the DTA to measure the heat flow under the constant flow of dry nitrogen gas as the temperature increased from 40°C to 800°C at a rate of 5°C/min.

X-ray diffraction patterns of the synthesized dry powders are shown in Fig. 1. Presence of weak xrd peaks corresponding to possibly Bi and Te (or Se) phases can be noticed in addition to the apparent XRD peaks from $Bi_2Te_3$ (or $Bi_2Se_3$) phases, representing that the chemical reactions did not proceed completely leaving small amounts of Bi and Te (or Se) phases in the final reaction products. However, majority of the final products are $Bi_2Te_3$ or $Bi_2Se_3$ as intended. Peak positions for the bulk $Bi_2Te_3$ and $Bi_2Se_3$ phases are indicated in Fig. 1 below the experimentally measured patterns with the powder diffraction file numbers of the phases. Measured patterns exhibited all the peaks corresponding to the bulk phases indicating that the crystalline structures of the synthesized particles were identical to those found in the corresponding bulk phases.

SEM micrographs in Fig. 1(b) and 1(d) confirm the development of 2D platelets during the chemical reactions for both $Bi_2Te_3$ and $Bi_2Se_3$, respectively. Hexagonal shape of the plates denotes the single crystalline nature of the synthesized nanoplates and their chemical compositions were also examined with energy dispersive spectroscopy (EDS) results (not shown here). In addition to the nanoplates, irregular shaped nanoparticles were observed and identified as residual Te or Se particles. After 24 hours of reaction, $Bi_2Se_3$ nanoplates exhibited greater widths in general compared to the $Bi_2Te_3$ plates. A bright-field TEM image of an individual $Bi_2Te_3$ plate and the diffraction patterns in the inset of Fig. 2(a) confirm that the platelet is indeed single crystalline with hexagonal symmetry. High resolution TEM image in Fig. 2(b) shows the lattice fringes of the $Bi_2Te_3$ nanoplates with the spacing of approximately 0.22 nm, which is close to the known value of

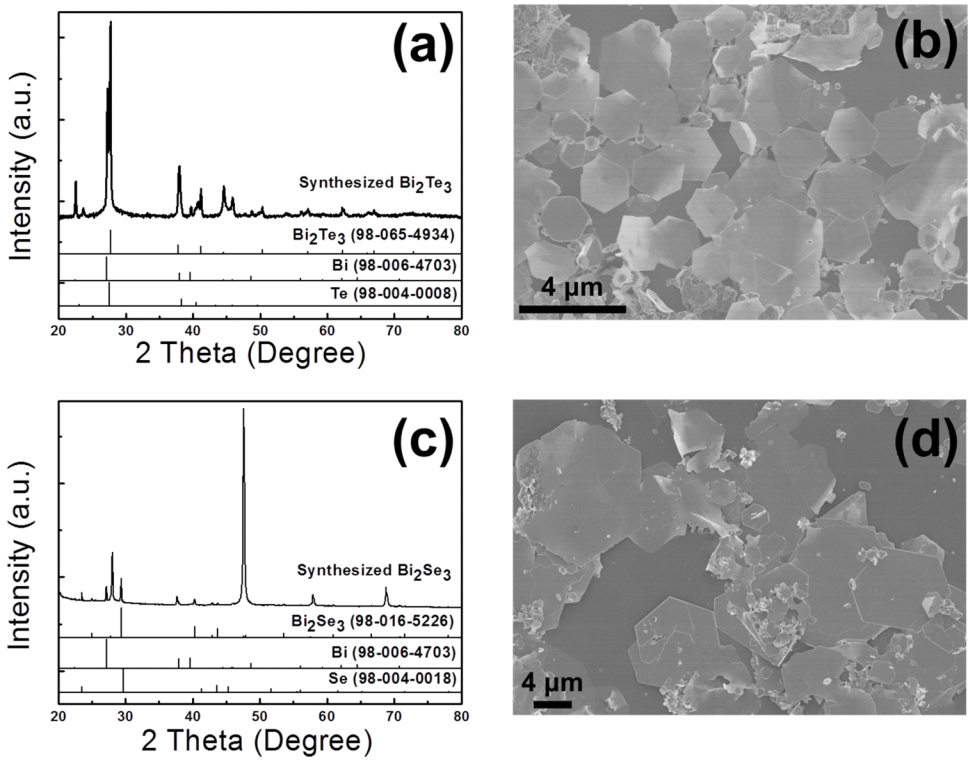


FIG. 1. XRD patterns and SEM micrographs of synthesized nanoplates. (a) and (b) are for $Bi_2Te_3$, and (c) and (d) are for $Bi_2Se_3$.

(110) lattice parameter, $d_{110}$ (= 0.219 nm). Elemental mapping results in Fig. 2(c)-2(d) exhibiting uniform distribution of Bi and Te atoms within the nanoplate also confirm the formation of $Bi_2Te_3$ with intended chemistry and hexagonal crystalline structure. Analogous TEM analyses were also obtained for $Bi_2Se_3$ nanoplates.

From the SEM observations of many nanoplates at various angles with the incident electron beam, widths of the plates were measured to be in the order of micrometer range while the thickness is in the order of nm range. In order to study the correlation between the morphology of the nanoplate and the amount of PVP added in the reaction bath, widths and thicknesses of many nanoplates synthesized at various PVP molarities were measured. Average widths and thicknesses of the $Bi_2Te_3$ nanoplates were extracted and plotted as a function of PVP molarity. Width of the nanoplates varied from approximately 1 to 6 μm. During the syntheses reactions, PVP is expected to adsorb on the polar {0001}surfaces of the nanoplate, which then suppresses further growth along the *c*-axis direction while the growth along the *a*-axis is not affected.[22,23] As shown in Fig. 3, measured average thickness of the nanoplates was indeed found to depend on the added amount of PVP. On the contrary, the width is almost unaffected by the PVP. Therefore, the aspect ratio defined as the width/thickness can be close to 190, which appears to be the highest among the $Bi_2Te_3$ nanostructures reported in previous literatures.[24–26] On the contrary, when PVP was not present in the reaction, it was verified that $Bi_2Te_3$ grew into irregular particle shapes rather than in the platelets. As PVP concentration increased over 0.5 mmol, the effect saturated and further thinning effect was not observed.

Although the crystal structure of the nanoplates was the same as the structure of the bulk, it is rational to expect the new or unexpected properties from the size and shape of the nanomaterials.[11] With this in consideration, thermal properties of synthesized nanoplates were tested with differential thermal analysis (DTA). For comparison, empty sample holder made of quartz was measured first as shown in Fig. 4(a), and 20 mg of $Bi_2Te_3$ commercial powders of a few μm in diameters purchased from Alfa Aesar Inc. were also measured. The result from the commercial powder showed an endothermic melting peak at 586°C (Fig. 4(b)), which is consistent with the known melting

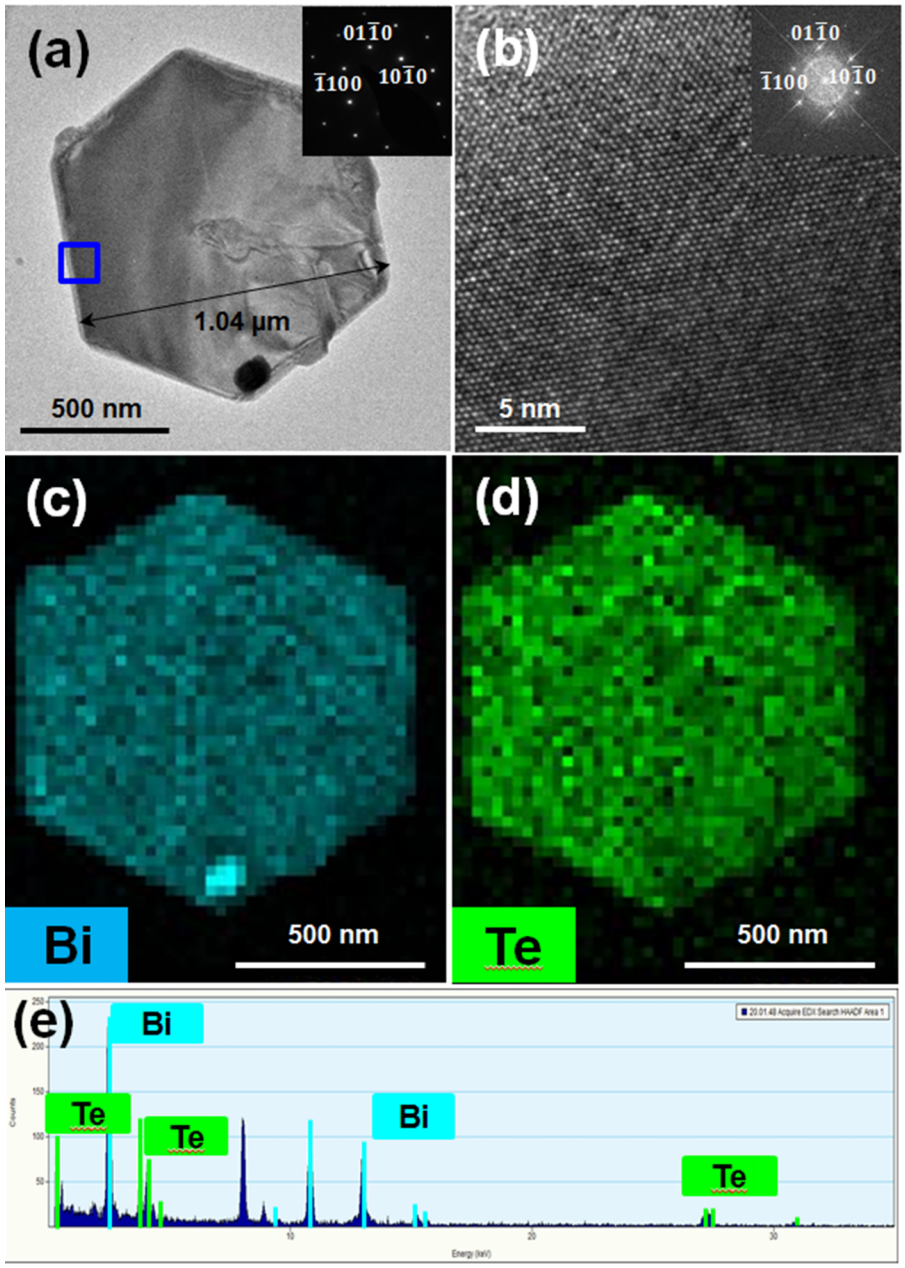


FIG. 2. (a) TEM image of the $Bi_2Te_3$ nanoplate synthesized by a solvothermal method. (b) A HRTEM image of the nanoplate shows the lattice images of the (0001) basal plane. Elemental maps show the distribution of (c) Bi atoms in blue color and (d) Te atoms in green color. (e) EDX data obtained from the nanoplate indicate that Bi and Te atomic concentrations are 38.91% and 61.09%, respectively.

temperature of bulk $Bi_2Te_3$. In comparison, the measurement with the synthesized nanoplates of $Bi_2Te_3$ in Fig. 4(c) gave the broad bump at temperatures ranging from 400°C to ~570°C. A tiny peak at 271°C was identified as the melting of the residual Bi phase. Residual Te is also expected to yield a tiny peak at around 450°C. Although the result is not a conventionally expected sharp peak, this may suggest the possibility of reduced melting temperature of $Bi_2Te_3$ by more than 150°C. This significant reduction of melting temperature is thought to be mainly due to the atoms at the surface of nanoplates. With the nanoplatelet shapes as shown in Fig. 1(b) and 1(d) with the lateral dimension of ~2 μm and the thickness of ~12 nm, surface to volume ratio is calculated to be over

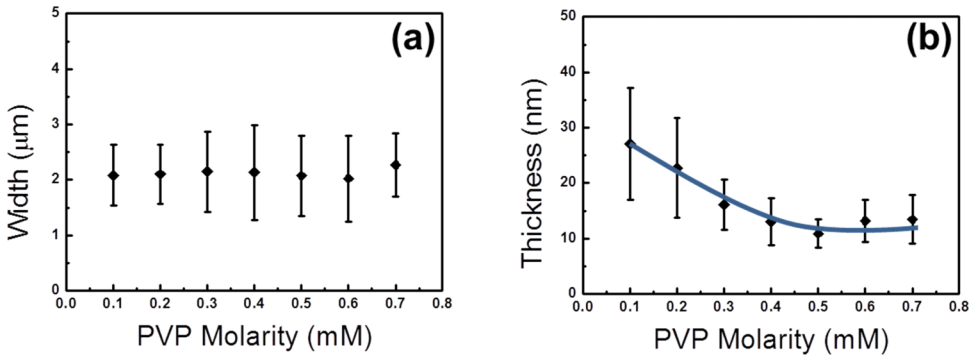


FIG. 3. Average width and thickness of the nanoplates were plotted as a function of PVP concentration in the reaction pot.

~166 $\mu m^{-1}$, while the spherical particles of the identical volume would have the surface to volume ratio of ~14 $\mu m^{-1}$. Therefore, by the formation of highly anisotropic shape of nanoplate, more than one order higher fractions of atoms are exposed to the surface, where the atoms can be freed more easily than in the bulk crystalline structure, thereby effectively reducing the melting temperature of the nanostructured materials.[27]

It is also noted that the measured melting appears to occur across the broad range of temperatures. This might be due to the facts that the nanoplates included in the measured specimen exhibit various thicknesses and that the melting temperature of a nanoplate is expected to depend on its thickness. Thinnest nanoplates in the specimen begin to melt first and the melting continues gradually with relatively thicker plates as the specimen temperature increases.

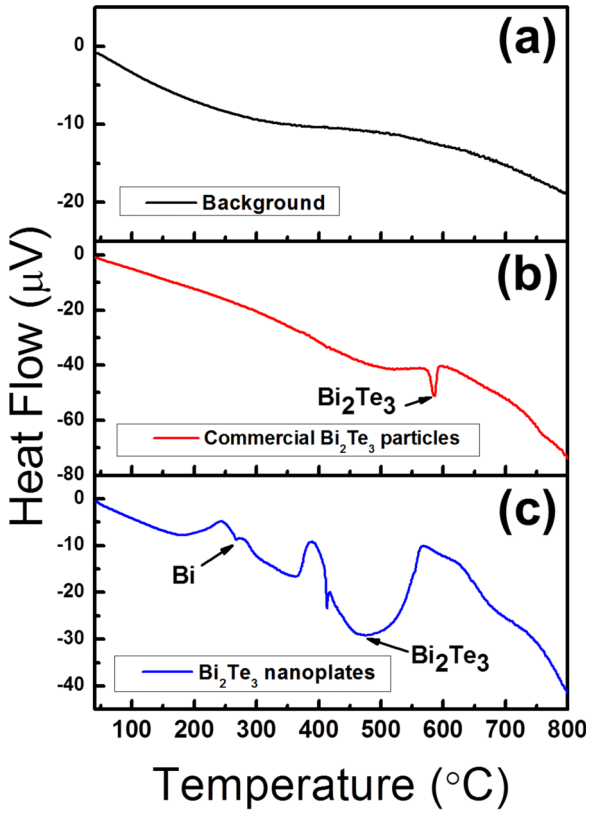


FIG. 4. (a) Empty $SiO_2$ sample holder was measured as the background. (b) DTA result of commercial $Bi_2Te_3$ particles with the endothermic peak at 586°C. (c) DTA result of the synthesized $Bi_2Te_3$ nanoplates.

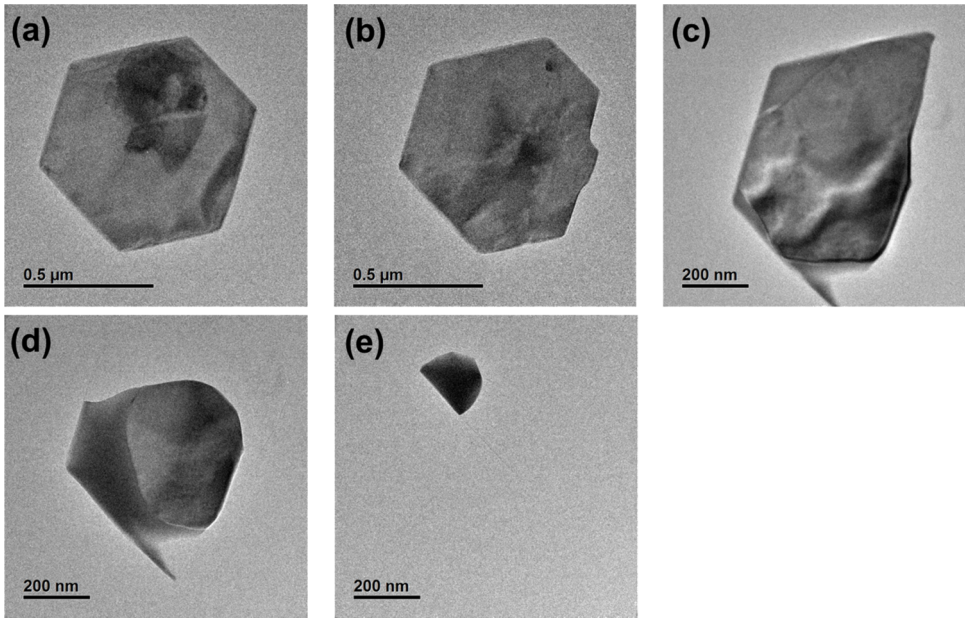


FIG. 5. TEM images of a $Bi_2Te_3$ nanoplate on a heating stage at (a) room temperature of 25°C. Micrographs were taken at 450°C after (b) 1 min 40 sec, (c) 4 min 20 sec, (d) 6 min 6 sec. (e) Temperature was increased to 490°C and 8 min elapsed.

For the clearer and more direct verification of the implications from the DTA measurement results, hexagonal $Bi_2Te_3$ nanoplates were mounted on the TEM heating stage and the thermal behavior was directly observed using the TEM as the specimen was heated from room temperature to ~500°C. Fig. 5(a) shows the hexagonal platelet at room temperature. As the temperature rose above 400°C, hexagonal plates began to shrink due to the melting followed by evaporation, mainly on the $\{10\bar{1}0\}$ side facets, representing much lower thermal stability for the nanoplates compared

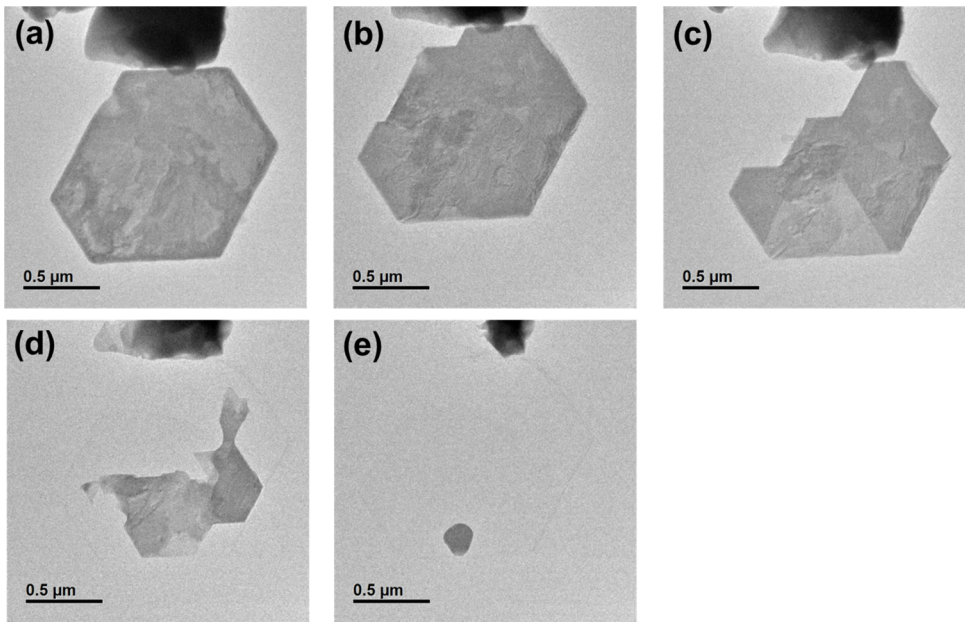


FIG. 6. TEM images of a $Bi_2Se_3$ nanoplate (a) taken at 25°C. Images were taken (b) after 1 min 40 sec at 550°C, (c) after 5 min 20 sec at 585°C, (d) after 40 sec in 600°C, and (e) after temperature was decreased to 550°C from 600°C for 2 min.

to the bulk $Bi_2Te_3$ with its nominal melting temperature of 586°C. At the temperature of 450°C, as shown in Figs. 5(b)-5(d), the nanoplate was already observed to have shrunken to a size of approximately one forth of the initial size. When the temperature was further increased to 490°C (in Fig. 5(e)), the width of the plate reduced to ~150 nm but did not disappear completely. This behavior at a temperature range between 400°C and 500°C appears to be consistent with the result obtained from DTA in Fig. 4. Similar behavior was also confirmed with $Bi_2Se_3$ nanoplate as shown in Fig. 6 with its melting and evaporation beginning at ~550°C, which is again considerably lower than the bulk melting temperature of $Bi_2Se_3$, 710°C. And, these occur over a broad range of temperatures. These results suggest the significant decrease in thermal stabilities of 2D nanoplates due to the reduced thickness in nanometer scale.

In summary, with the PVP adsorptions on the polar basal planes of $Bi_2Te_3$ and $Bi_2Se_3$ structure during the initial stage of chemical syntheses, asymmetrical growth of nanostructure was demonstrated to produce 2D nanoplates. Possibility of thickness control in the nanoplates was confirmed by adjusting the amount of added PVP. And, it was found that the thermal stability is drastically suppressed in the nanoplates than in the bulk counterpart based on the DTA and TEM experiments. This means that the reduction of melting temperature can be caused by the reduced size in *only one of the three spatial dimensions* rather than the reduction of overall size in three dimensions as was usually assumed for the cases of nanoparticles.

## ACKNOWLEDGMENTS

Authors thank the financial support of DGIST HRHR program from DGIST and RISE program from GIST. Fundings from the Korean National Research Foundation (NRF) with the grant numbers of 2012K1A4A3053565, 2014R1A2A2A01003709 and 2013R1A1A1007978 are also acknowledged.

[1] M. Brust, M. Walker, D. Bethell, D. J. Schiffrin, and R. Whyman, J. Chem. Soc., Chem. Commun **7**, 801 (1994).
[2] J. H. Fendler and F. C. Meldrum, Adv. Mater. **7**, 607 (1995).
[3] S. Iijima, Nature **354**, 56 (1991).
[4] P. Yang, R. Yan, and M. Fardy, Nano Lett. **10**, 1529 (2010).
[5] K. S. Novoselov, A. K. Geim, S. V. Morozov, D. Jiang, Y. Zhang, S. V. Dubonos, I. V. Grigorieva, and A. A. Firsov, Science **306**, 666 (2004).
[6] B. Radisavljevic, A. Radenovic, J. Brivio1, V. Giacometti, and A. Kis, Nat. Nanotechnol. **6**, 147 (2011).
[7] D. Teweldebrhan, V. Goyal, and A. A. Balandin, Nano Lett. **10**, 1209 (2010).
[8] D. Kong, W. Dang, J. J. Cha, H. Li, S. Meister, H. Peng, Z. Liu, and Y. Cui, Nano Lett. **10**, 2245 (2010).
[9] Ph. Buffat and J. P. Borel, Phys. Rev. A **13**, 2287 (1976).
[10] M. Maillard, S. Giorgio, and M. –P. Pileni, J. Phys. Chem. B **107**, 2466 (2003).
[11] A. P. Alivisatos, Science **271**, 933 (1996).
[12] X. Peng, L. Manna, W. Yang, J. Wickham, E. Scher, A. Kadavanich, and A. P. Alivisatos, Nature **404**, 59 (2000).
[13] J. I. Hong, J. Choi, S. S. Jang, J. Gu, Y. Chang, G. Wortman, R. L. Snyder, and Z. L. Wang, Nano Lett. **12**, 576 (2012).
[14] A. Salant, M. Shalom, Z. Tachan, S. Buhbut, A. Zaban, and U. Banin, Nano Lett. **12**, 2095 (2012).
[15] H. Li, X. Qi, J. Wu, Z. Zeng, J. Wei, and H. Zhang, ACS Nano. **7**, 2842 (2013).
[16] S. –W. Min, H. S. Lee, H. J. Choi, M. K. Park, T. Nam, H. Kim, S. Ryu, and S. Im, Nanoscale **5**, 548 (2013).
[17] P. Hu, L. Wang, M. Yoon, J. Zhang, W. Feng, X. Wang, Z. Wen, J. C. Idrobo, Y. Miyamoto, D. B. Geohegan, and K. Xiao, Nano Lett. **13**, 1649 (2013).
[18] D. Kim and J. Moon, Electrochem. Solid-State Lett. **8**, J30 (2005).
[19] S. Jeong, K. Woo, D. Kim, S. Lim, J. Kim, H. Shin, Y. Xia, and J. Moon, Adv. Funct. Mater. **18**, 679 (2008).
[20] J. Perelaer, P. J. Smith, D. Mager, D. Soltman, S. K. Volkman, V. Subramanian, J. G. Korvink, and U. S. Schuber, J. Mater. Chem. **20**, 8446 (2010).
[21] Y. Liang, W. Wang, B. Zeng, G. Zhang, J. Huang, J. Li, T. Li, T. Song, and X. Zhang, J. Alloys. Comp. **509**, 5147 (2011).
[22] Y. Xu, Z. Ren, W. Ren, G. Cao, K. Deng, and Y. Zhong, Mater. Lett. **62**, 4273 (2008).
[23] H. He, D. Huang, X. Zhang, and G. Li, Solid State Commun. **152**, 810 (2012).
[24] G. Zhang, W. Wang, X. Lu, and X. Li, Cryst. Growth & Des. **9**, 145 (2009).
[25] Y. Xu, Z. Ren, G. Cao, W. Ren, K. Deng, and Y. Zhong, Mater. Lett. **62**, 4525 (2008).
[26] Y. Zhang, L. P. Hu, T. J. Zhu, J. Xie, and X. B. Zhao, Cryst. Growth & Des. **13**, 645 (2013).
[27] W. H. Qi and M. P. Wang, Mater. Chem. Phys. **88**, 280 (2004).